Probing buried magnetic nanostructures by spin-resolved local density of states at the surface: A density functional study

O. O. Brovko,[1] V. S. Stepanyuk,[1] W. Hergert,[2] and P. Bruno[3]

[1]*Max-Planck-Institut für Mikrostrukturphysik, Weinberg 2, D06120 Halle, Germany*
[2]*Fachbereich Physik, Martin-Luther-Universität, Halle-Wittenberg, Friedemann-Bach-Platz 6, D06099 Halle, Germany*
[3]*European Synchrotron Radiation Facility, BP 220, F38043 Grenoble Cedex, France*

We demonstrate that it is possible to resolve magnetic properties of small clusters buried up to 1.5 nm deep beneath a metallic surface. The possibility of deducing magnetic properties of buried nanostructures by studying polarization maps of the surface is discussed. Moreover, we show that there is a way to determine the coupling of buried structures to each other by studying the polarization of electrons in vacuum space above the system.

I. INTRODUCTION

Nowadays, as scientists and engineers aspire to create high-density magnetic storage with a unit size approaching that of a single atom, the prospect of using arrays of sub-surface magnetic impurities as storage grids becomes more and more appealing. Recently it has become possible to carry out charge switching of single impurities buried up to 1 nm below a semiconductor surface[1] which proves the aptitude of modern experimental techniques for addressing properties that were previously only accessible to theoretical studies. Another example of such a property is the magnetic moment of a buried impurity, which may provide even more flexibility for engineering purposes. As a consequence, the importance of finding a way to directly probe the buried structure's magnetism can hardly be underestimated.

Already from the earliest stages of the history of surface nanoscience the subject of buried structures and interfaces has been of considerable interest to both experimentalists and theoreticians. Early scanning tunneling microscopy (STM) and spectroscopy (STS) experiments have shown that it is possible to detect electronic states of bulk impurities embedded several layers deep into a metallic[2] and semiconductor[3] surfaces. Manifestations of subsurface gas impurities in the STM spectra[4] were reported and Friedel (or Ruderman-Kittel) oscillations around dopant sites in semiconductors[3] were observed. These effects were closely investigated both experimentally and theoretically[4–7] and have been extensively utilized in a subsequent series of studies to determine the electronic structure and position of subsurface impurities[8,9] as well as to study buried interfaces and lattices.[10]

Only recently, after the initial submission of the present paper, the interest in sub-surface STM studies has been reinflamed by a publication of Weismann *et al.*[11] that clearly demonstrated that it is possible to study buried impurities by means of an STM and utilize them as Fermi-surface probes, nanosonars, spin filters, or exchange interaction adjustment tools. However, to our knowledge, the issue of probing the impurity's magnetism has up to now never been directly addressed. The scope of magnetism studies was confined to such areas as the Kondo effect at embedded magnetic

atoms[12] and spin-dependent scattering at buried interfaces (see, for example, Ref. 13).

In the present paper we demonstrate the possibility to directly probe the magnetism of nanostructures buried in metallic surfaces. Our *ab initio* calculations reveal a pronounced dependence of the local density of electronic states (LDOS) in vacuum above the embedding site of a cluster on its burying depth. Moreover strong spin-selective features of this dependence give rise to equally pronounced variations in the polarization of electrons at the surface, which oscillates with increasing burying depth reaching both large positive and large negative values. We present the calculated in-plane polarization maps at the surface above magnetic clusters embedded at various depths into the surface. We show that such maps can allow one to judge about the burying depth of an embedded nanostructure as well as to determine its electronic and magnetic properties. To emphasize the importance of the approach we present calculations for pairs of buried clusters which suggests a way to deduce the magnetic coupling between them by analyzing the polarization of the surface caused by their presence.

II. *AB INITIO* APPROACH DETAILS

In our calculations we utilize the Korringa-Kohn-Rostoker (KKR) Green's function method in atomic-spheres approximation.[14,15] This method is an implementation of the density-functional formalism in local spin-density approximation. The KKR approach utilizes the properties of the Green's function of the Kohn-Sham operator allowing the electronic density to be expressed through the imaginary part of the energy-dependent Green's function of the system. The Dyson equation allows us to obtain the Green's function of an arbitrary system as a perturbation of a simpler one with a known Green's function.[16] We treat a surface as a two-dimensional (2D) perturbation of an ideal crystal bulk with a slab of vacuum. Taking into account the translational symmetry of the surface geometry, the Green's functions are formulated in momentum space. Buried clusters and atoms are considered as the perturbation of the clean surface. These calculations for embedded structures are performed in real space. In all further mentions of calculations in vacuum
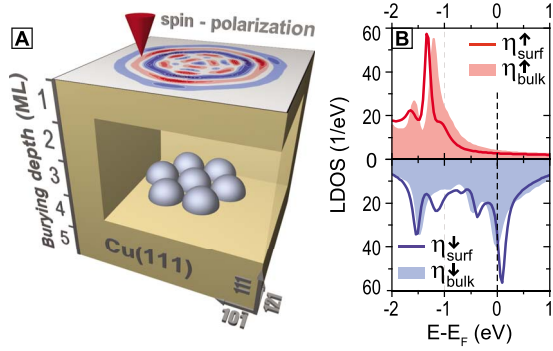
FIG. 1. (Color online) (a) The sketch of the studied system—a hexagonal Co cluster of seven atoms (H7) buried in a Cu(111) surface. (b) Majority [light red (light gray) filled area] and minority [light blue (dark gray) filled area] LDOS in of the central atom of the cluster embedded in Cu bulk. Majority [red (light gray) solid curve and minority [blue (dark gray) solid curve] LDOS of the central atom of the cluster embedded into the topmost layer of a Cu(111) surface.
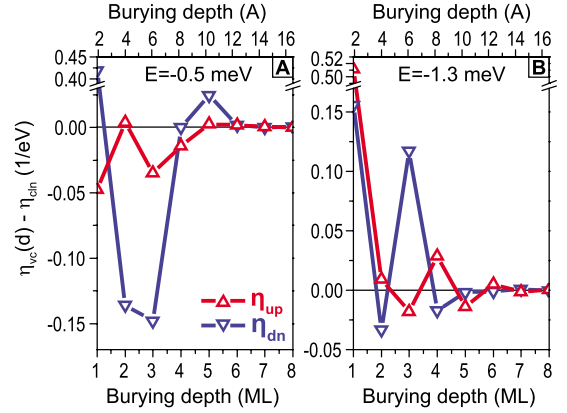

FIG. 2. (Color online) Majority [red (light gray) triangles up] and minority [blue (dark gray) triangles down] LDOS at (a) −0.5 and (b) −1.3 eV in vacuum above the embedding site of an H7 Co cluster versus the burying depth. The LDOS of a host surface has been subtracted from all the curves for clarity.

above the burying site calculations for the first vacuum layer some 2 Å above the surface are implied. The choice of the distance was governed solely by considerations of the calculational convenience. In an actual STS experiment, where the typical tip-substrate separations lie in range of 5−10 Å, the measured differential conductance values would be lower, as the electronic density of a certain state decays exponentially into the vacuum.

III. RESULTS AND DISCUSSION

As a model system for our investigations we have chosen a Co cluster consisting of seven atoms arranged in the shape of a hexagon all residing in the same layer beneath a Cu(111) surface. It has been shown[17] that such magnetic systems can be produced by buffer-layer-assisted growth and subsequent capping-layer deposition. The investigated burying depths ranged between 1 (surface layer) and 8 monolayers (ML) which corresponds to about 2−17 Å. Figure 1(a) contains a sketch of the system. The electronic structure of the central atom of the Co cluster is presented in Fig. 1(b). The filled curves represent the majority [red (light gray)] and minority [blue (dark ray)] LDOS in the case of a cluster embedded in Cu bulk. Due to interactions within the cluster the degeneration is lifted from atomic states resulting in the formation of several peaks in each LDOS channel. The most prominent peaks lie at −1.45, −0.44, and 0.0 eV for minority, and at −1.6 and −1.2 eV for majority electrons. As the burying depth is reduced and the cluster approaches the surface, the peak positions, and intensities change finally reaching the values represented by solid red (light gray) (majority) and blue (dark gray) (minority) curves in Fig. 1(a) which correspond to a cluster embedded into the topmost layer of a Cu(111) surface.

Now let us consider how the buried nanostructure affects a quantity which is accessible to us at the surface, namely, the LDOS. Selecting two energies (−1.3 and −0.5 eV) each corresponding to a region containing a prominent peak in

either the majority or the minority LDOS of the cluster let us trace how the LDOS at the surface changes as we gradually increase the burying depth. Figure 2(a) shows the majority [red (light gray) triangles pointing up] and minority [blue (dark gray) triangles pointing down] LDOS at −0.5 eV in vacuum above the embedding site of the cluster as a dependence of the burying depth. A similar burying depth dependence for the LDOS at −1.3 eV is presented in Fig. 2(b). The reference LDOS of a clean surface has been subtracted from the curves to reveal the partial influence of the submerged impurity on the electronic density. It can be seen that both majority and minority LDOS display an oscillatory behavior. To understand the physics behind the phenomenon we might consider the following. The strongly localized nature of atomic d orbitals of the cluster's atoms prevents them from affecting the LDOS at the surface directly. However the s electrons of the metallic host, scattered at atomic orbitals can propagate through the overlayer. After reaching the surface the electrons are scattered at the vacuum barrier. The oncoming and reflected electrons then interfere with each other. The interference, depending on the impurity's burying depth and the k vector of the electrons in question, can have either a constructive or a destructive character which either increases or decreases the density of states at the surface. Thus changing the burying depth we change the interference conditions and with them the LDOS at the surface.

Moreover, due to inherent polarization of atomic states, different behavior of the majority and minority LDOS with increasing cluster burying depth can be observed. This results in polarization of the surface electrons throughout the LDOS spectrum. As an example Fig. 3 displays the polarization of electrons at the surface as a function of energy and burying depth [$P=P(E,d)$]. It is plain that the oscillations of the LDOS with increasing burying depth cause the polarization to oscillate accordingly. The values of the polarization reach both large positive and large negative values ranging between +35 and −50%. The polarization can be traced up to the burying depths of at least 8 ML ($\sim$17 Å). Thus it is clear that the polarization along with the LDOS is a very sensitive
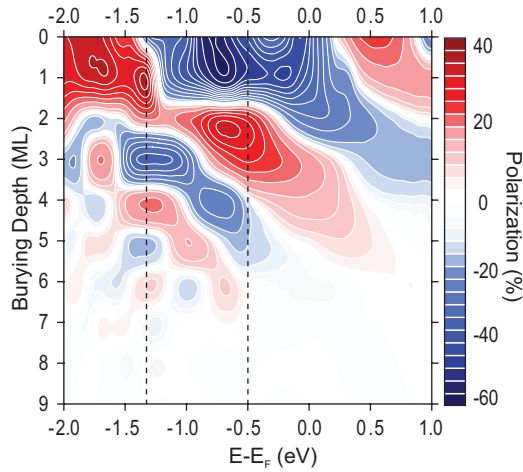
FIG. 3. (Color) Polarization (color coded) $P=P(E,d)$ above a buried hexagonal 7-atomic Co cluster as a function of electron energy and burying depth. The $P(E)$ distributions have been calculated for integer layer numbers and then interpolated for clarity. The dashed vertical lines mark the energies chosen for comparison.

tool for studying embedded magnetic nanostructures.

There are still several questions that have to be addressed. One of the most profound ones is how the behavior of the polarization changes if we alter the geometry of the cluster, for example, by increasing its size. To clarify this issue let us compare the behavior of the polarization above a 7-atomic cluster (H7) to that above a 19-atomic hexagonal one (H19). And as an asymptotic case for our comparison let us take a polarization above a complete Co monolayer buried at the same depths as the clusters. Figure 4 displays the polarization above buried H7 (black rectangles), and H19 [red light gray) circles] clusters as well as that above a buried monolayer (blue triangles) as a function of burying depth at our chosen energies of (a) −0.5 and (b) −1.3 eV (marked with dashed lines in Fig. 3). It is notable that at larger burying depths, when the distance to the surface is much larger than the extents of both H7 and H19 islands, the corresponding curves display a very similar behavior while at smaller depths when the size of the islands comes into play the behavior of the curves start to differ. Moreover it can be noted
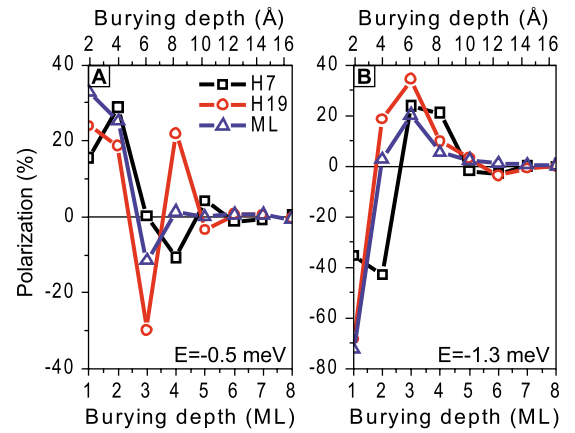

FIG. 4. (Color online) Comparison of the polarization at the surface above buried 7-atomic (H7, black squares), 19-atomic [H19, red (light gray) circles] clusters, and a buried monolayer [ML, blue (dark gray) triangles pointing up] at (a) −0.5 eV and (b) −1.3 eV. The lines are meant solely as a guide for the eyes.

that up to a depth of 6–7 Å the H19 curve bears a much closer qualitative resemblance to the ML one which indicates that at shallow burying depths the H19 influences the surface polarization in a way very similar to a complete monolayer's.

Incidentally, the fact that at larger burying depths the size of the island ceases to affect the behavior of the polarization at the surface helps us resolve another issue. It is well known (see, for example, Ref. 18) that small metallic clusters at surfaces often exhibit super paramagnetic properties which might impede the experimental application of the ideas discussed here. However, by increasing the size of the clusters it should be possible to achieve sufficient values of magnetic anisotropy to sustain a constant direction of the magnetic moment at a reasonable experimental environment temperature.

Thus it is clear that already by studying just a single point above a buried nanostructure we can gain important, though limited, information about the structure's burying depth and also gain some insight into its electronic and magnetic properties. However, to acquire more information about the system in whole it might be useful to consider not only a single point but an in-plane distribution of the polarization in
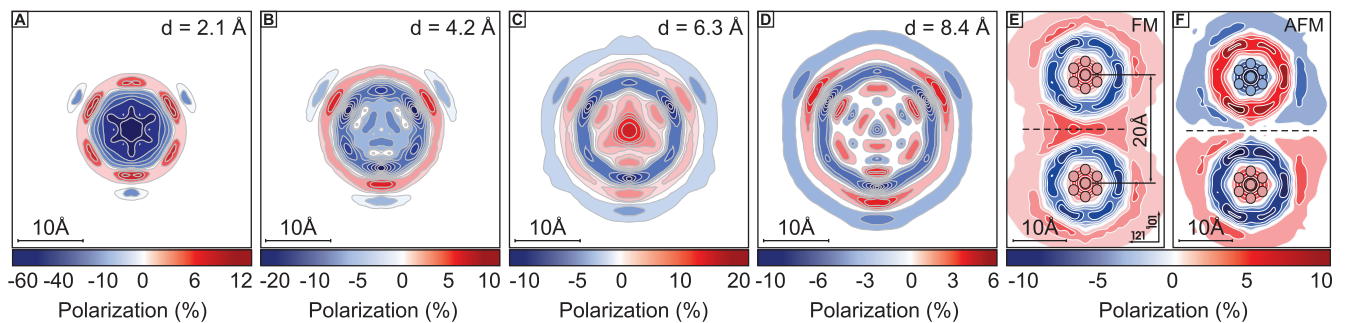

FIG. 5. (Color) Polarization maps above a hexagonal 7-atomic cluster of Co residing under a Cu(111) surface at burying depths of (A) 2.1, (B) 4.2, (C) 6.3, and (D) 8.4 Å. Polarization above a pair of H7 clusters of Co buried in the same layer 6.3 Å deep beneath a Cu(111) surface with a center-center separations of 20 Å and either a parallel (E) or antiparallel (F) alignment of clusters' magnetic moments. Red and blue circles denote the burying sites of Co atoms with spin pointing up and down, respectively. Dashed lines mark the symmetry plane of the system. All the maps are plotted for the electrons at −0.5 eV.

vacuum above the nanostructure's burying site. Figure 5 shows calculated polarization-distribution maps at −0.5 eV in vacuum above an H7 clusters buried in monolayers 1 to 4 (A–D, respectively) beneath the surface. At each burying depth the cluster produces a unique polarization-distribution signature in the vacuum space above its burying site. Following the intrinsic properties of a (111) surface the polarization maps display a threefold rotational symmetry. Looking at the polarization distributions one once again detects the characteristic details of the electronic interference, namely, the radially propagating oscillations of polarization. They are also easy to understand. As we stray from the center of the system the distance to the buried nanostructure is increased and consequently the phase relations of interfering incoming and scattered electronic waves change causing the resulting periodic variations in the polarization of surface electrons. Note also that with increasing burying depth the radial period of the oscillations decreases which complies with simple notions of wave optics. The phase of the oscillations is determined by the electronic properties of the host material of the surface as well as by the burying depth of the impurity. Consequently, the phase and the period of in-plane radial oscillations of the polarization can provide us with important information about the position and the burying depth of an embedded nanostructure. Mapping the subsurface structure's polarization could also allow one to determine to some extent its geometrical properties, for example by fitting the polarization distribution with a simple multiple-scattering model.

If subsurface structures are to be considered as candidates for magnetic storage devices, the understanding of the nature of their interaction has to be reached and a way has to be found to effectively probe the interaction between single buried nanostructures. Let us consider a pair of H7 clusters of Co buried in the same layer 6.3 Å deep beneath a Cu(111) surface with a center-center separation of 20 Å. Atomic spins inside Co clusters are known to align themselves parallel to each other. The relative alignment of the two clusters' spins is, on the contrary, *a priori* unknown and depends on many factors, such as the islands' relative position and the host material of the surface. The polarization distribution on the surface above the two clusters is presented in Figs. 5(e) and 5(f) for the case of parallel (FM) and antiparallel (AFM) orientation of clusters' magnetic moments, respectively. The system with a FM alignment of moments has produced a polarization map which is a superposition of two similar distributions set of by 20 Å. The AFM system, on the contrary,

produced a map which is perfectly antisymmetrical with respect to the symmetry plane $(\bar{1}01)$ separating the buried structures [marked by a dashed line in Figs. 5(e) and 5(f)]. Such a behavior can easily be understood if we consider that in a system with AFM orientation of moments the electrons scattered at majority states of one cluster will interfere with electrons scattered at minority states of the other thus creating an antisymmetrical distribution. Thus it can be said that the symmetry of the polarization map can be regarded as a signature of the relative moment orientation of the buried clusters. Moreover, it can be noted that the antisymmetrical polarization distribution implies the absence of polarization along the symmetry plane which might be regarded as an additional and even simpler criterion of the clusters' moments alignment. Thus, the polarization maps can be utilized to determine the coupling of nanostructures buried up to 15 Å deep beneath a metallic surface.

IV. OUTLOOK AND CONCLUSIONS

Before we proceed to conclusions it should be noted here that the goal of the present work was not to precisely mimic experimental measurements but rather to introduce and discuss the general idea. Should this topic motivate a further experimental study, the theoretical investigation should be extended to include the calculation of geometries matching the experimental ones and the results should be formulated (for easier comparison) in terms of spin-resolved differential conductivity based on the Tersoff-Hamman model.[19]

In conclusion, we have shown that magnetic properties of nanostructures buried up to 15 Å beneath a metallic surface can be deduced from the spin-resolved local density of states above the surface. We believe that such measurements can be carried out by means of a conventional spin-polarized STM. Acquiring in-plane polarization maps in vacuum above the surface can allow one to simultaneously detect electronic, magnetic, and even geometric properties of sub-surface structures. The coupling of buried nanostructures to each other can be deduced from the symmetry of the polarization map.

[1] K. Teichmann, M. Wenderoth, S. Loth, R. G. Ulbrich, J. K. Garleff, A. P. Wijnheijmer, and P. M. Koenraad, Phys. Rev. Lett. **101**, 076103 (2008).

[2] S. Heinze, R. Abt, S. Blügel, G. Gilarowski, and H. Niehus, Phys. Rev. Lett. **83**, 4808 (1999).

[3] M. C. M. M. van der Wielen, A. J. A. van Roij, and H. van Kempen, Phys. Rev. Lett. **76**, 1075 (1996).

[4] M. Schmid, W. Hebenstreit, P. Varga, and S. Crampin, Phys. Rev. Lett. **76**, 2298 (1996).

[5] K. Kobayashi, Phys. Rev. B **54**, 17029 (1996).

[6] S. Crampin, J. Phys. Condens. Matter **6**, L613 (1994).

[7] S. Heinze, G. Bihlmayer, and S. Blügel, Phys. Status Solidi A **187**, 215 (2001).

[8] Y. S. Avotina, Y. A. Kolesnichenko, A. N. Omelyanchouk, A. F. Otte, and J. M. van Ruitenbeek, Phys. Rev. B **71**, 115430 (2005).

[9] C. Didiot, S. Vedeneev, Y. Fagot-Revurat, B. Kierren, and D. Malterre, Phys. Rev. B **72**, 233408 (2005).

[10] I. B. Altfeder, D. M. Chen, and K. A. Matveev, Phys. Rev. Lett. **80**, 4895 (1998).

[11] A. Weismann, M. Wenderoth, S. Lounis, P. Zahn, N. Quaas, R. G. Ulbrich, P. H. Dederichs, and S. Blugel, Science **323**, 1190 (2009).

[12] N. Quaas, M. Wenderoth, A. Weismann, R. G. Ulbrich, and K. Schönhammer, Phys. Rev. B **69**, 201103(R) (2004).

[13] Y. Xu, X. Mi, Y. Z. Wu, and K. Xia, Phys. Rev. B **76**, 184431 (2007).

[14] K. Wildberger, V. S. Stepanyuk, P. Lang, R. Zeller, and P. H. Dederichs, Phys. Rev. Lett. **75**, 509 (1995).

[15] R. Zeller, P. H. Dederichs, B. Újfalussy, L. Szunyogh, and P. Weinberger, Phys. Rev. B **52**, 8807 (1995).

[16] J. Zabloudil, R. Hammerling, L. Szunyogh, and P. Weinberger, *Electron Scattering in Solid Matter*, Springer Series in Solid-State Sciences Vol. 147 (Springer-Verlag, Berlin, 2005).

[17] M. A. Torija, A. P. Li, X. C. Guan, E. W. Plummer, and J. Shen, Phys. Rev. Lett. **95**, 257203 (2005).

[18] J. Xu, M. A. Howson, B. J. Hickey, D. Greig, E. Kolb, P. Veillet, and N. Wiser, Phys. Rev. B **55**, 416 (1997).

[19] J. Tersoff and D. R. Hamann, Phys. Rev. B **31**, 805 (1985).